Fast and Rigorous BoR FDTD Algorithm for the Modelling of Coupled EM-Thermal Processes in Axisymmetrical Devices

Lukasz Nowicki[1], Malgorzata Celuch[1], Marzena Olszewska–Placha[1], Janusz Rudnicki[1]

[1]QWED Sp. z o. o., Krzywickiego 12, 02078 Warsaw, Poland,
email:lukasznowicki@qwed.eu

Keywords: Microwave Heating, Electromagnetic Heating, Multiphysics Modelling, Numerical Techniques, Computational Electromagnetics, Heat Flow, Batteries, Computer Aided Design.

I. Motivation and background

Computational modelling has been gaining increasing interest of the microwave heating community and as such, it has become a regular topic of AMPERE conferences. While this paper is not meant as a review, let us refer the reader to two papers of AMPERE 2001, subsequently archived [1][2], for more historical references including relevant background and perspectives for further developments. In particular, it can be seen that the works on microwave power modelling follow two paths: identification and re-use of pre-existing computational tools [1], originally developed for other microwave technologies such as telecommunication and radar, and development of dedicated modelling workflows [2], which take the nonlinear processes as the focus. Additionally, benchmark examples have been defined [3], which allow meaningful verification and comparison of commercial and in-house modelling tools without revealing industrial secrets of the reference microwave applicator designs [1][3][4]. A review chapter [4] summarises the state-of-the-art in the use and development of the currently leading FDTD (Finite-Difference Time-Domain) and FEM (Finite Element) Methods, including accuracy and efficiency comparison of four popular commercial software packages (QuickWave and CST – for FDTD, COMSOL and HFSS – for FEM) for an open benchmark after [3] as well as a commercial domestic microwave oven.

The starting point for our work reported herein is an observation that the works as in [1-4] consider microwave heating problems in their full 3D (three-dimensional) representation. While such an approach in always correct, it is not always computationally efficient. If the structure of interest contains geometrical symmetries, exploiting such symmetries in the computer model accelerates the simulation by several orders of magnitude, without any loss of accuracy or physical information, which is incorporated analytically [5]. Of specific interest in microwave technologies are axially symmetrical problems, such as coaxial components [6] and satellite communication antennas [5]. Also in the area of microwave heating, axisymmetrical applicators are relevant to, e.g., timber drying [7]. In our H2020 NanoBat project [8], the specific interest was on the modelling of electromagnetic (EM) heating in batteries, many of which are in practice cylindrical. This has stimulated our work to couple the Bodies-of-Revolution (BoR) formulation of the FDTD method for Maxwell equations [5][6] with an analogous BoR FDTD for heat flow equations. Let us note that this requires casting the equations into the cylindrical coordinate system. While the operation appears in principle straightforward, its practical implementation it requires solving specific mathematical problems due to e.g. on-axis singularities [9], which influence stability and efficiency of the algorithm. In the available literature on thermal modelling, this has been obviated by either ignoring the cylindricity of the system and keeping the differential operators in their Cartesian forms (which approximates the reality far away from the axis, but is unacceptable for small-radius problems and effects, e.g. in batteries) or by requiring manual coordinate transformations by the user [10]. In our work, a rigorous BoR FDTD formulation for coupled EM-heat flow equations has been developed based on the approach of [6][9]. The transformation of coordinates is included in the code and therefore transparent to the user. The achieved computational efficiency improvements, with respect to the brute-force 3D modelling, are by over a factor of 100, as shown by the examples below. No physical information is lost, no mathematical pre-processing is required on the user's side.

II. Coupled electromagnetic and thermal simulation of axisymmetrical microwave process

Heat transfer refers to the exchange of energy in the form of heat between bodies or environments that are at different temperatures. This transfer can occur through conduction, convection, or radiation. The second laws of thermodynamics dictate that over time, temperature differences within a closed system will become more uniform as heat is transferred from hotter areas to cooler ones. This homogenisation process is accompanied by the movement of heat flux from high-temperature areas to low-temperature areas, with the rate of heat flux increasing as the temperature difference between the two points becomes larger. Using heat transfer theory, the differential equation for heat transfer shows how temperature is distributed continuously with respect to both spatial and time coordinates, allowing for the solution of heat conduction problems. Process of conducting FDTD analysis starts with sinusoidal excitation to obtain the electromagnetic steady-state. The analysis is then used to produce a 3D pattern of average dissipated power in lossy

material. The enthalpy per cell is then upgraded using the average power and a-defined time of heating in seconds, resulting in an updated enthalpy density. Next, the temperature distribution in each FDTD cell is updated.

As one of the implementation example, a model imitating a popular AAA battery [11] is chosen. Thus, the model is a cylinder with a length of 49.5 mm and a radius of 9.5 mm filled with lossy material through the centre of which passes a cathode rod of 1.25 radius (Fig.1). A common electrolyte is chosen as the loss material; Lithium hexafluorophosphate (LiPF6) salt with a concentration of 0.5 mol/kg dissolved in dimethyl carbonate (DMC). At this concentration, as shown in [12], conductivity hardly increases with temperature. For this reason, it has been assumed that it is constant and its value has been set to 0.2 S/m. The relative permittivity also does not change and is equal to 3.1075. In order to take advantage of the capabilities of the heating module, we also enter thermodynamic material parameters such as: density of 1.29 g/cm3, specific heat of 0.1339 J/(g°C) and thermal conductivity equal to 0.0045 W/(cm°C). These values are taken from [13].

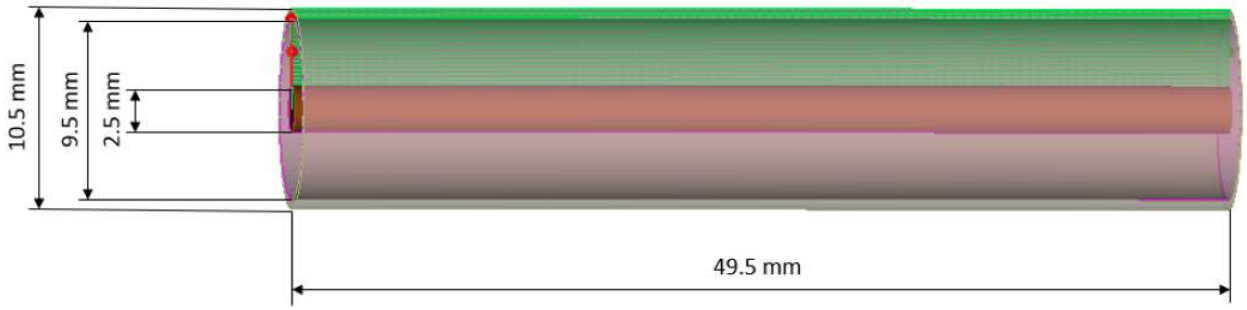

Fig. 1. Dimensions of the considered model of the popular AAA battery.

Two models are considered, for which accuracy and efficiency will be compared: classical full 3D and BoR developed in this work. In both models, the meshing in the axial direction is set to 0.5 mm while 0.1 mm is used in the cross-section (of which only the radial direction is discretised in the BoR model) (Tab. 1). To generate a steady state, the models are bounded by a source and a load and excited by a sinusoidal TEM field. Here, the frequency of 2.45 GHz is used for compatibility with ISM microwave applications and in the range of GHz technologies explored in [8] for battery materials' testing. The simulation begins with an FDTD EM analysis of the battery model up to the EM steady-state. Based on it, a template of average power dissipation values is calculated. The enthalpy value in each FDTD cell is then updated. All the material parameters defined above are used to obtain the temperature distribution. These results are provided to the heat transfer module HFM, where FDTD thermal calculations are run by solving the heat flow equations with adiabatic boundary conditions. After its completion, it returns the final temperature, enthalpy, and dissipated power distributions.

Table 1. The final parameters of the electromagnetic and heat flow simulation procedure performed for the battery model.

Calculations method	BoR FDTD			3D		
	Simulation time (min:sec)	Iterations	Number of cells	Simulation time (min:sec)	Iterations	Number of cells
EM	0:04	17647	11948	0:54	20504	1212516
HFM	0:08	1764		1:36	2050	

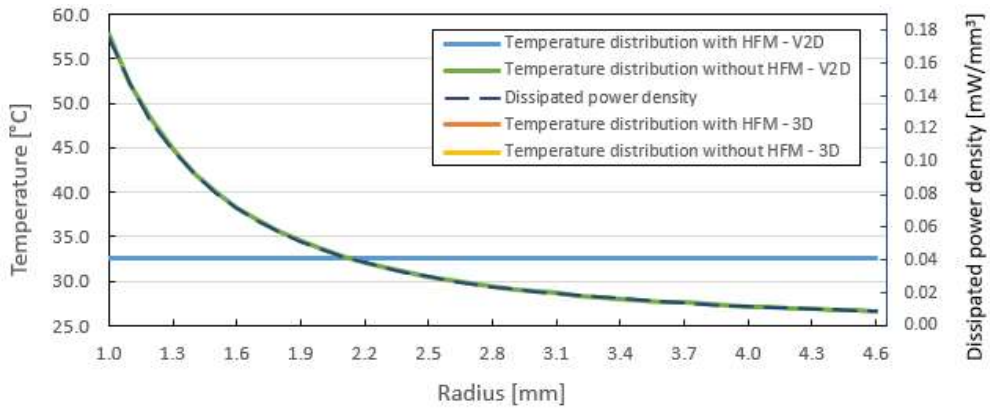

Fig. 2. Temperature distribution for heating simulations without and with flow with adiabatic boundary conditions in the radial direction (on the inner and outer conducting electrode) at an initial temperature of 25 °C – BoR and 3D results overlap.

To study the speed of the thermal calculations and their influence on the overall computing effort, nonzero electrical losses and thermal conductivity are set only over a section of the electrolyte, of increasing thickness. An increase in the thickness increases the simulation time although for the BoR FDTD model it is only a few seconds (Tab. 2). The dissipated power density is the same for both cases, BoR and 3D (Fig. 2), and as analytically expected, in the radial direction it is inversely proportional to radius squared. In the pure EM model, without heat flow, the temperature distribution follows the dissipated power distribution pattern. When heat flow is included, after the HFM stage, the temperature distribution is uniform in the radial direction, as shown in Fig. 2. All curves resulting from BoR simulations coincide with those from 3D (Fig. 2) but are obtained after much shorter simulation times - economies are by an order of magnitude for this small model and increase with model size (Table 1).

Table 2. Simulation times obtained after the heating procedure with the heat flow module for different electrolyte thicknesses of the BoR FDTD and 3D model with adiabatic boundary conditions.

Thickness of electrolyte [mm]	BoR FDTD Simulation time (min:sec)	3D Simulation time (min:sec)
1	0:08	0:59
10	0:10	1:06
20	0:10	1:39
30	0:11	2:03
40	0:12	2:21

III. Extension to a nonlinear microwave process in axisymmetrical resonators

In this section, the previous BoR FDTD algorithm with a heat flow module will be extended with an algorithm for automatic updating of material parameters as a function of temperature, following the methodology proposed for 3D simulations in [2]. Additionally, we shall explain how an FDTD algorithm, which is deterministic by nature, is applied to solving eigenvalue problems in microwave resonators.
For illustration, a microwave heating device model based on the patent of [16] will be presented. The device of [16] is designed to heat disk-shaped objects containing different amounts of water. The device is shown in Fig. 3. It uses an antenna connected to a coaxial cable to introduce energy into the load. The device itself is designed to produce TM_{011} wave patterns, TM_{010} wave patterns, or a combination of the two, depending on the object's dielectric constant. The applicator's dimensions are carefully selected to meet two conditions: to create cylindrical TM_{011} resonance and to generate a TM_{010} field pattern when not in resonance. Figure 2 shows the dimensions of the considered applicator calculated based on the recommendations in [16] and assuming its operation close to the ISM frequency of 2.45 GHz. Then from equation (1) for the obtained radius, the frequencies for TM_{010} and TM_{011} modes are analytically calculated as 2.13 GHz and 2.44 GHz. The TM_{01} mode is the second mode (of the second lowest cutoff frequency) to propagate in a circular waveguide, with the TE_{11} mode being the fundamental mode (of the lowest cutoff frequency). Each mode is evanescent below its cutoff frequency, while above the cutoff frequency it propagates with a well-defined propagation constant. The cutoff frequency is dictated by the waveguide radius r and modal numbers m, n:

$$f_{c,TMmn} = \frac{c}{2\pi}\frac{\chi_{m,n}}{r}, \qquad (1)$$

where f_c is the cutoff frequency [Hz], c is the speed of light in vacuum [m/s], r is the radius of the waveguide [mm] and $\chi'_{m,n}$ is n-th root of m-th Bessel function. For TE modes, the root $\chi_{m,n}$ of the Bessel function is replaced by the root $\chi'_{m,n}$ of the function's derivative.

We first create a pure EM model and simulate it with BoR FDTD. We aim to solve an eigenvalue problem in the cylindrical applicator, confirming the analytically pre-calculated eigenfrequencies. To this end, we eliminate the feeding structure (coaxial line in Fig. 2a) and simulate only the cylindrical. Since FDTD is in itself a deterministic method, we need to approximate the eigenvalue problem by a resonant deterministic problem. We do so by inserting a virtual point source connected to a longitudinal E-field node close to the axis of rotation. Fig. 4 shows the Fourier transform of the current flowing through such a virtual point source – the minima indicate the resonances (in accordance with the physical sense of the resonance). Both resonances seen in Fig. 4 (2.13 GHz and 2.44 GHz) well approximate the analytically calculated ones – the discrepancy is caused by numerical dispersion and decreases with refined FDTD discretization.

The resonator is then modelled together with the feeding coaxial line. Now, minima of abs(S11) indicate the resonances of the actual heating device. Since the coupling is small, they are similar to the resonant frequencies calculated with the

virtual point source. Then a lossy material with a thickness of 5 mm is placed in the applicator (as indicated in Fig. 3a). As a consequence the resonant frequencies are shifted downward.

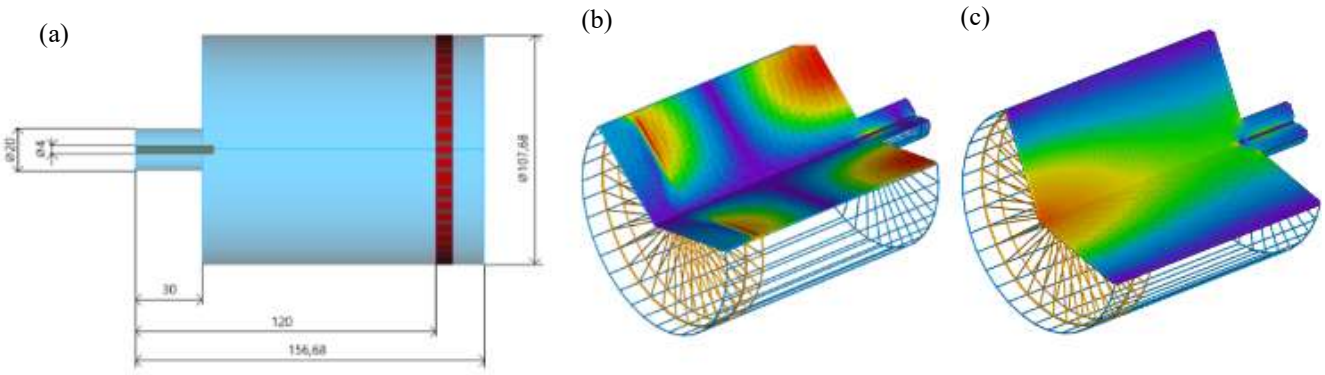

Fig. 3. Considered microwave applicator, it's (a) dimensions after [16] and distribution of the (b) magnetic field and (c) electric field of the TM_{011} mode, in a 270 degree view of the cylinder.

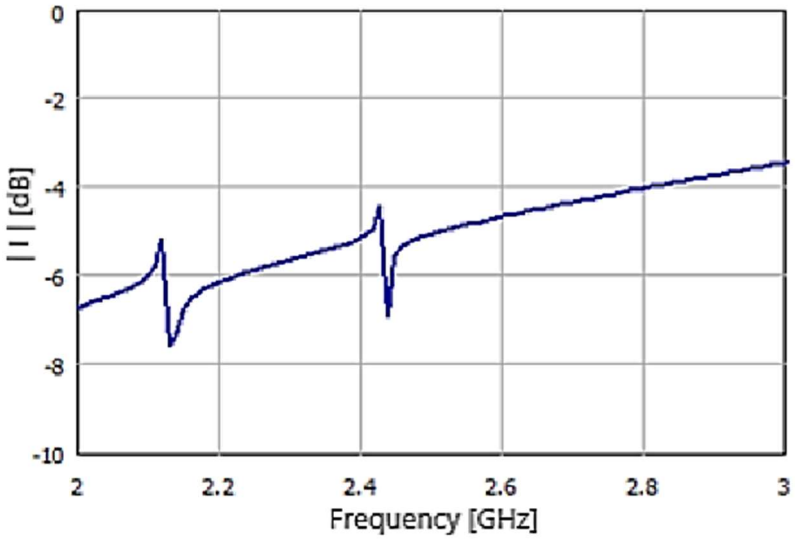

Fig. 4. Current flowing between the auxiliary point source and the resonator.

Apart from the frequency response, another crucial factor to consider a model of microwave oven is uniformity of heating of the materials being processed. The lossy material placed in the applicator has temperature-dependent material parameters defined. These are updated at the end of the heating step.

The simulations uses a source with a sinusoidal TEM excitation at 2.13 GHz. The meshing is uniform in both directions and is 1 mm. One of the heated objects is bread, whose parameters are defined as temperature-independent constants. The electrical conductivity is equal 0.221 S/m and the effective permittivity is 4.17 after [7]. The final heating time is 120 seconds with different time steps as in the legend in Fig.6. The simulation assumes an initial temperature of -20 °C. Using BoR FDTD when calculating EM steady in each case simulation takes only one second. What it can be notice at Fig. 6 is that when we increase the number of steps during heating the bread including the heat flow module, the temperature doesn't go up so quickly. This happens because we are splitting the total power delivered over 120 seconds into smaller parts. That means there are more instances of heat flow during the simulation. If you focus on a differences in temperature distributions of different heating steps (Fig.5). It can be notice that the temperature across the bread doesn't change significantly anymore. This means that the temperature distribution becomes more stable. This information helps us figure out the best balance between simulation time and the accuracy final results. This is also confirmed by the Fig. 6, where for steps of 5 and 10 seconds they begin to converge. However, it should be taken into account that linear interpolation is used to draw the lines, between successive heating steps. Note that the number of steps is really important when the material undergoes dynamic changes in its properties.

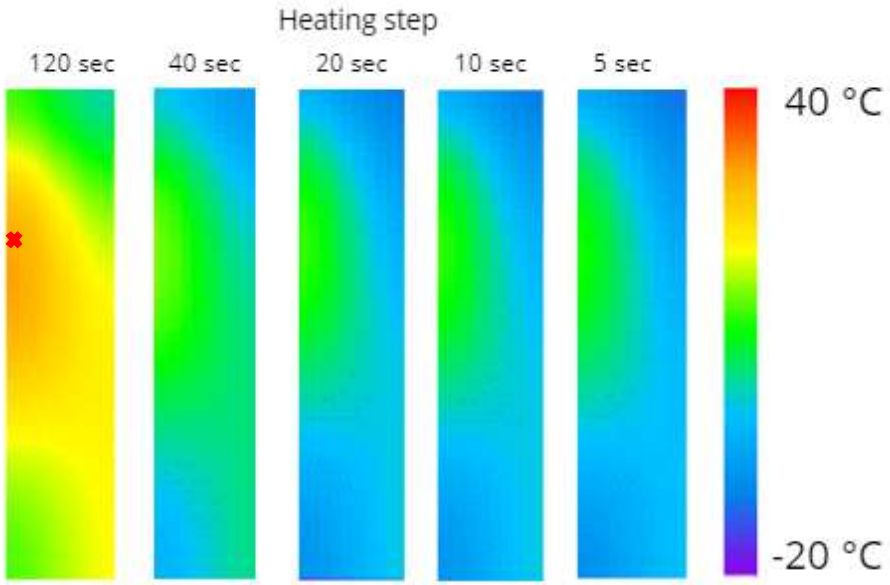

Fig. 5. Distribution of final temperature in bread after heating for 120 sec, including heat flow phenomenon – parameterised simulations using different heating steps. Red spot means hot spot in bread.

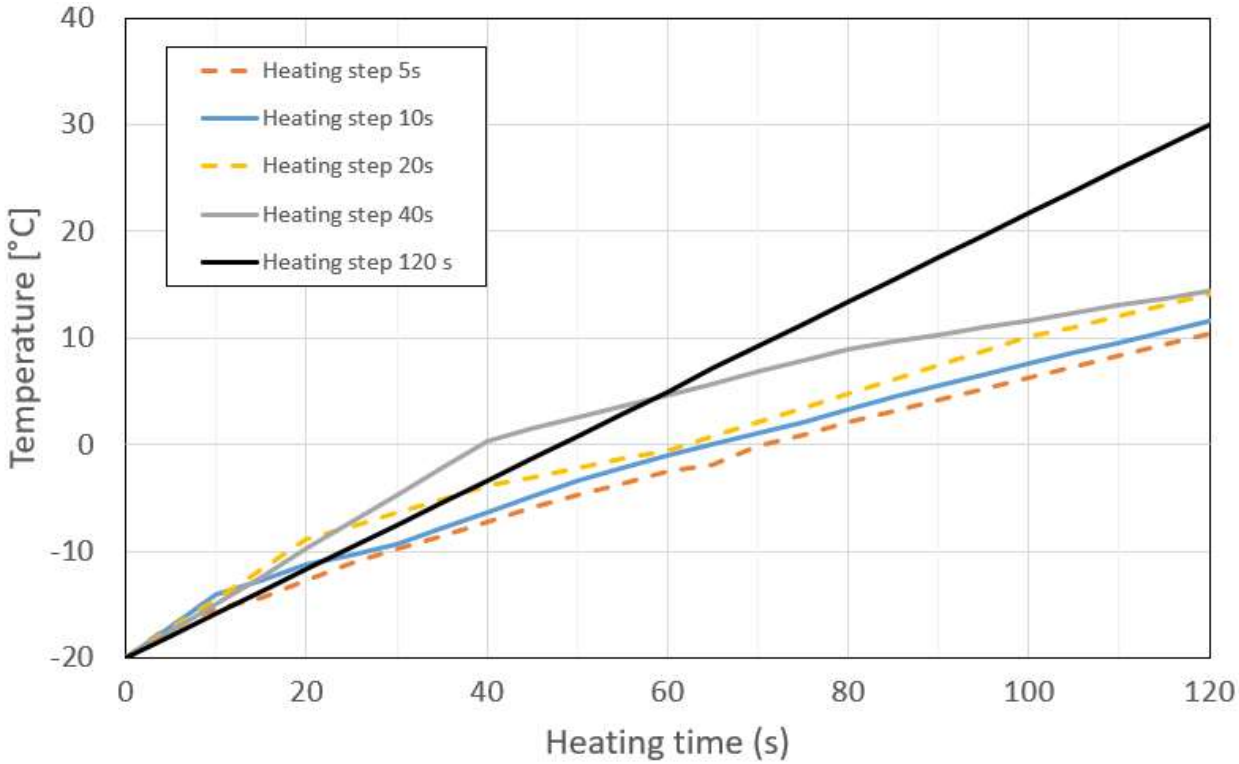

Fig. 6. Comparison of temperature evolution in simulated bread hot spot in heating simulations including heat flow.

The second material considered is beef whose parameters depend significantly on temperature. Parameters are also as in [17]. The relative permittivity changes from 4.9 to 41.7 in the temperature range from -20 to 80 °C. In the same range, its conductivity changes from 0.064 to 2.426 S/m maximum conductivity, which occurs in the -1 °C. Consequently, the power dissipated is most effectively absorbed by the beef causing, that is, an increase in temperature. However, an interesting relationship can be seen when the hot spot is examined, in these cases the maximum temperature at each step was taken into account. For beef, the temperature distributions are shown after heating (120 seconds) taking into account the heat flow phenomenon (Fig. 7) and with this step of the heating procedure like in Fig. 5. The increase in temperature in the beef causes significant changes in conductivity. If we set a step of 120 seconds, so one step is taken, all the power lost in the beef will be calculated on the initial parameters. Reducing the heating step of the simulation causes a hot spot to appear. It was marked with a red cross and the maximum temperature values were taken from there. Based on them, lists of such values were created for heating mode with and without flow calculations (Fig. 8) for beef.

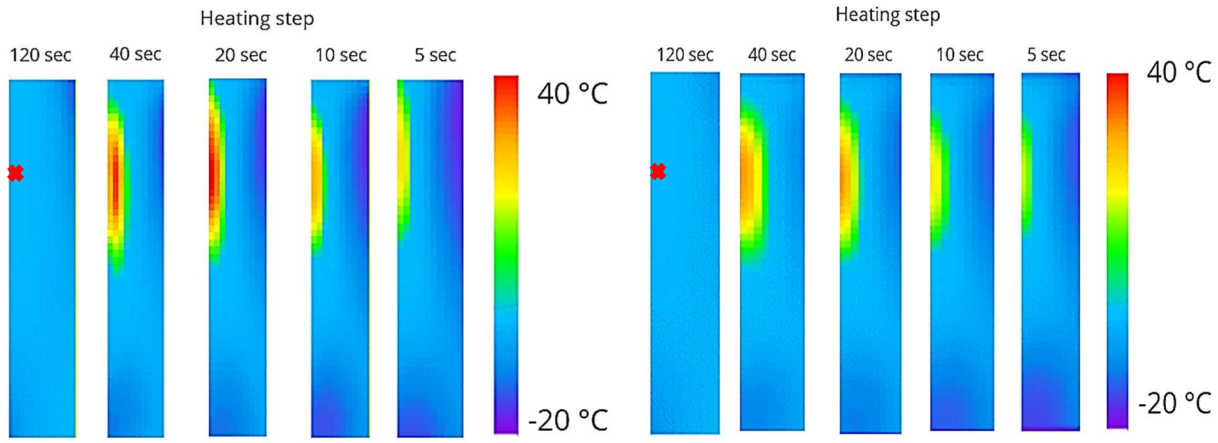

Fig. 7. Distribution of final temperature in beef after heating for 120 seconds (a) heat flow neglected (b) including heat flow phenomenon. Parameterised simulations using different heating steps. Red spot means hot spot in beef.

When beef gets to around -1 °C its properties start changing significantly. It is important to mention that Fig. 8 shows that after 120 seconds, the values for BHM and BHM+HF are a bit different by 0.02 °C. The curves that come together at the 60-seconds mark for all steps are because of how much the material properties matter. See, between -2.2 and -1 **°C**, there are 5 different temperatures where the material's permittivity and conductivity change. Conductivity goes up by about 1 S/m, and permittivity increases by a significant 19 points. This means there's some uncertainty in choosing the right step.

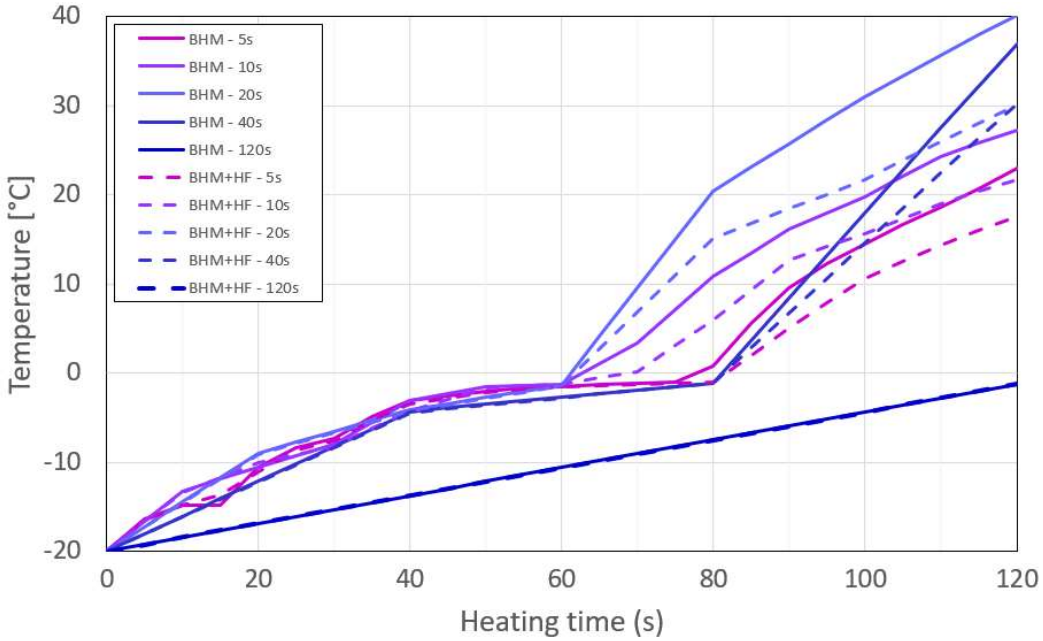

Fig. 8. Comparison of temperature evolution in simulated beef hot spot in with and without considering heat flow with different simulation time step.

IV. Conclusions and future work

The Bodies-of-Revolution FDTD algorithm has been extended from pure electromagnetic to coupled nonlinear EM-thermal problems including heat flow phenomena. Compared with 3D modelling, significantly lower simulation times have been demonstrated for the BoR approach. For more complex models, the difference will definitely be more noticeable. A cylindrical microwave heating applicator has been considered as an EM eigenvalue and deterministic problem, and then as a multiphysics problem. Based on the AAA battery model, the algorithm was verified for a linear problem with adiabatic boundary conditions. The nonlinear problem is parameterised by dividing the microwave heating time into heating steps, with EM parameters of all materials assumed constant during each such step, but changed

automatically by the software in each FDTD cell separately, between each two heating steps, in accordance to the local temperature of each cell.

Further work is ongoing on including charge transport mechanisms in the multiphysics problem. In the realm of battery industries, incorporating charge transport mechanisms and coupled electrochemical models into electromagnetic testing tools is crucial for accurate characterization and understanding of energy materials, such as those used in Li-ion batteries, facilitating advancements in battery research and technology. The developed solvers as well as a representative examples are made available on the Open Platform of NanoBat [8] and I4Bags [17] projects, which aims develop processing and characterisation of battery applications. More results will be presented at the conference.

Acknowledgement: The reported work received funding from the European Union's Horizon 2020 research and innovation programme under grant agreement NanoBat No 861962. Currently the work of QWED team receives funding from the Polish National Centre for Research and Development under M-ERA.NET3/2021/83/I4BAGS/2022.

References

[1] V.V. Yakovlev, “Examination of contemporary electromagnetic software capable of modeling problems of microwave heating”, in: Advances in Microwave and Radio Frequency Processing: Report from 8th International Conference on Microwave and High-Frequency Heating (Bayreuth, 2001), ed. M. Willert-Porada, Springer, Berlin, 2006, pp. 178-190.
[2] M. Celuch-Marcysiak, W.K. Gwarek, and M. Sypniewski, „A novel FDTD system for microwave heating and thawing analysis with automatic time-variation of enthalpy-dependent media parameters”, in: Advances in Microwave and Radio Frequency Processing: Report from 8th International Conference on Microwave and High-Frequency Heating (Bayreuth, 2001), ed. M. Willert-Porada, Springer, Berlin, 2006, pp. 199-209.
[3] P.O.Risman, “A microwave oven model - examples of microwave heating computations”, Microwave World, vol.19, No.1, Summer 1998, pp.20-23.
[4] M. Celuch, P. Kopyt, and M. Olszewska-Placha, ”Modeling of cavities and loads with FDTD and FEM methods”, Ch. 18 in: Development of packaging and products for use in microwampereave ovens" , eds. U. Erle, P. Pesheck, and M. Lorence, Elsevier, 2020, pp. 459-511.
[5] M. Celuch and W. K. Gwarek, "Industrial design of axisymmetrical devices using a customized FDTD solver from RF to optical frequency bands", IEEE Microwave Mag., vol. 9, No. 6, pp. 150-159, Dec. 2008.
[6] W.K. Gwarek, “Computer-aided analysis of arbitrarily-shaped coaxial discontinuities”, IEEE Trans. Microwave Theory Tech., vol.36, pp. 337-342, Feb. 1988.
[7] P.O.Risman and M.Celuch-Marcysiak, "Electromagnetic modelling for microwave heating applications", invited paper, Proc. 13th Intl.Conf. on Microwaves, Radar and Wireless Communications MIKON-2000, Wroclaw, May 2000, vol.3, pp.167-182.
[8] (2023) H2020 NanoBat Open Modelling Platform [Online]. Available: https://www.qwed.eu/nanobat2.php
[9] M. Celuch-Marcysiak and W.K. Gwarek, "Improved and simpler FDTD formulation for axisymmetrical problems", Proc.2000 IEEE-AP-S International Symp. and USNC/URSI National Radio Science Meeting, Salt Lake City, Utah, US, July 2000, vol.1, pp.228-231.
[10] T. Kindo, “Guidelines for Equation-Based Modeling in Axisymmetric Components”, (2023) COMSOL Blog. [Online]. Available: https://www.comsol.com/blogs/guidelines-for-equation-based-modeling-in-axisymmetric-components/
[11] Energizer product datasheet, https://data.energizer.com/pdfs/e92.pdf
[12] E. R. Logan,1 Erin M. Tonita, K. L. Gering, Lin Ma,Michael, K. G. Bauer, Jing Li, L. Y. Beaulieu and J. R. Dahn “A Study of the Transport Properties of Ethylene Carbonate-Free Li Electrolytes” ” Journal of The Electrochemical Society, 165 (3) A705-A716 (2018), March 2018
[13] David R. Lide, ed., CRC Handbook of Chemistry and Physics, Internet Version 2005, <http://www.hbcpnetbase.com>, CRC Press, Boca Raton, FL, 2005. If a specific table is cited, use the format: "Physical Constants of Organic Compounds", in CRC Handbook of Chemistry and Physics, Internet Version 2005, David R. Lide, ed., <http://www.hbcpnetbase.com>, CRC Press, Boca Raton, FL, 2005.
[14] W. J. R. Hoefer and P. P. M. So, The Electromagnetic Wave Simulator: A Dynamic Visual Electromagnetics Laboratory based on the Two-dimensional TLM Method, J.W.Wiley Software, 1991.
[15] A.Z. Elsherbeni and V. Demir, The Finite-Difference Time-Domain Method for Electromagnetics with MATLAB (R) Simulations, SciTech Publishing Inc., New York, 2016.
[16] Per O. Risman, Huskvarna, Sweden, Microwave Heating Apparatus, United States Patent, Appl. No.: 974,606,1981
[17] I4Bags Open Modelling Platform [Online] Available: https://qwed.eu/i4bags.html